

xxxx

xxxxxx

Advance Access Publication Date: Day Month Year

Manuscript Category

Subject Section

AMGC: Adaptive matching based genome compression

Jia Wang¹, Yi Niu^{1,2*}, Tianyi Xu¹, Mingming Ma¹, Dahua Gao¹ and Guangming Shi^{1,2}

¹ School of artificial intelligence, Xidian University, Xian, China 710071 and

² The Pengcheng Lab, Shenzhen, China, 518055.

* To whom correspondence should be addressed.

xxx

xxx

Abstract

Motivation: Despite significant advances in Third-Generation Sequencing (TGS) technologies, Next-Generation Sequencing (NGS) technologies remain dominant in the current sequencing market. This is due to the lower error rates and richer analytical software of NGS than that of TGS. NGS technologies generate vast amounts of genomic data including short reads, quality values and read identifiers. As a result, efficient compression of such data has become a pressing need, leading to extensive research efforts focused on designing FASTQ compressors. Previous researches show that lossless compression of quality values seems to reach its limits. But there remain lots of room for the compression of the reads part.

Results: By investigating the characters of the sequencing process, we present a new algorithm for compressing reads in FASTQ files, which can be integrated into various genomic compression tools. We first reviewed the pipeline of reference-based algorithms and identified three key components that heavily impact storage results: the matching positions of reads on the reference sequence (*refpos*), the mismatched positions of bases on reads (*mispos*) and the matching failed reads (*unmapseq*). To reduce their sizes, we conducted a detailed analysis of the distribution of matching positions and sequencing errors and then developed the three modules of AMGC. According to the experiment results, AMGC outperformed the current state-of-the-art methods, achieving an **81.23%** gain in compression ratio on average compared with the second-best-performing compressor.

Availability: <https://github.com/wj-inf/AMGC>

Contact: niuyi@mail.xidian.edu.cn

1 Introduction

Since the appearance of Next-Generation Sequencing (NGS) technologies (Mardis (2008)), we have witnessed the rapid development of sequencing technologies. Although Third-Generation Sequencing (TGS) technologies (Schadt *et al.* (2010)) have been widely developed, NGS technologies remain dominant in the current sequencing market for two main reasons. Firstly, the sequencing data produced by NGS technologies has a significantly lower error rate than that of TGS technologies. For example,

in the HiSeq (NGS technology) data, 92% of sequenced bases had a base quality score ≥ 30 , which means that the estimated error rate was less than 0.1% (Ma *et al.* (2019)). TGS long reads usually have high error rates: 15% with PacBio sequencing, and as high as 40% with Oxford Nanopore sequencing (Wee *et al.* (2019)). These high error rates make the assembly of TGS sequences seem disproportionately complex and expensive compared to the assembly of NGS sequences. NGS data also has richer analytical software. Tools like SAM tools (Li *et al.* (2009)), BWA-MEM and Bowtie2 (Li (2013)) have been widely used, making downstream analysis of NGS data more convenient. As a result, well-known companies Illumina and

BGI still regard NGS as an important sequencing business, especially Illumina's HiSeq sequencer series.

NGS technologies can generate massive amounts of sequencing data every day. For example, a NovaSeq 6000 sequencer can produce up to 3TB data in a single 44-hour run. However, the expansion of NGS data poses a serious challenge to its storage and transfer. How to effectively store and transmit these massive high-throughput genomic data has been a pressing issue. Genomic data compression technology becomes an important way to solve this problem. As there exist clear formats for read identifiers, the compression of NGS data focuses on short reads and quality values. According to previous research (Niu et al. (2022)), lossless compression of quality values seems to reach its limits. However, the compression of the reads part exists further potential.

In this work, we propose an algorithm for read compression, AMGC, which improves over the state-of-the-art compressors. AMGC consists of three key modules, aiming at solving three encoding redundancies in the current pipeline of reference-based approaches. The first module focus on the encoding of reference matching positions (*refpos*). By further analyzing the distribution of *refpos*, we discovered that adjacent reads are more likely to match close positions on the reference sequence and propose the bit-plane-based differential *refpos* encoding module. After that, we investigate the synthesis reaction involved in the NGS sequencing process and find that sequencing errors are more common in the trailing part of the short reads. This results in a uniform distribution of sequencing errors. To address this, we propose the adaptive binary mismatching positions encoding module. It uses a binary vector to denote matching mistakes and then encodes the vector using a high-order context. Finally, as the front subsegment has better quality than the rear subsegment, continuous mismatch bases in the trail may lead to the match fault of the whole read. Accordingly, we further propose the recursive split matching module. Read will be split into two segments after matching fault, and the two segments are aligned again. So the high-quality front subsegment could match successfully.

We evaluated AMGC on the datasets chosen from the standard test datasets provided by AVS-G. The experiment results showed that AMGC got an 81.23% average gain compared with the second-best-performing compressors with comparable RAM and time usage.

2 Related works

NGS technologies have produced large numbers of short genomic reads that are highly redundant and compressible. However, popular general-purpose compression tools such as *gzip*, *bzip2*, and *7z* can not achieve satisfactory performance on genome data. Because they do not take full advantage of the biological properties of the data, like repetitive fragments and palindromes. Therefore, efficient compression methods designed specifically for genome data are highly needed, bringing lots of significant work.

For the original FASTQ format, several specialized compression methods have been proposed (Bonfield and Mahoney (2013)) (Deorowicz and Grabowski (2011)). Based on whether additional reference genomes are required, these compression techniques can be broadly categorized into three groups: High-order context compression algorithms, assembly-based compression algorithms, and reference-based compression algorithms. High-order context compression algorithms are progressively being phased out.

Assembly-based approaches exploit the similarity between reads in FASTQ files and splice the measured short sequences into a long sequence by the assembly algorithm. They can deal with unsequenced species and macrogenomics, as they do not require a reference genome. Quip (Jones et al. (2012)) uses a Bloom filter to construct a de Bruijn graph for splicing. And the spliced contigs sequences are used as the reference genome for

sequenced reads in the original FASTQ file. Finally, only the aligning position and variation information of each sequenced read are recorded for coding. Leon (Benoit et al. (2015)) constructs a de Bruijn graph using all sequenced reads. Similar to the Quip method, Leon also uses a Bloom filter to filter out the low-abundance k-mer nodes to reduce the number of bifurcation nodes. Each sequenced read is represented as the path start node plus the fork node information. Then it is encoded in a tree structure and a zero-order context model, respectively. HARC (Chandak et al. (2018)) reorders reads roughly according to their position in the genome. These reordered reads are encoded to remove the redundancy between consecutive reads, and the parameters obtained are stored in different files. The files obtained above are compressed using Lempel-Ziv (Ziv and Lempel (1977)) and BWT (Burrows and Wheeler (1994)) based universal compressors. PgRC (Kowalski and Grabowski (2020)) constructs pseudogenomes, which are approximately the shortest common superstrings of reads. Then it encodes the reads according to their mapped positions on the pseudogenomes.

Reference-based approaches align the sequenced reads to an external reference sequence to identify similarities between them. Only the position of the comparison and variation information is encoded instead of the original target sequences. These methods achieve better performance by exploiting the similarity between the sequenced genome and the reference genome. Using the human genome as an example, over 99% of base pairs can be matched to the reference genome (Lander et al. (2001)). In LW-FQZip (Zhang et al. (2015)), reads are preprocessed by a lightweight mapping model and then mapping results are compressed by a general-purpose tool such as LZMA. Algorithms such as CRAM (Fritz et al. (2011)) employ a standard reference-based scheme to compress SAM/BAM data. This scheme relies on a highly optimized SAM field that supports various statistical models. The use of these models results in a reduction of the compression rate, as they can more efficiently capture the relevant information from the reference sequence. GTZ (Xing et al. (2017)) is a widely preferred reference-based algorithm in industrial applications. It performs significantly better than other previously proposed reference-based algorithms in terms of compression results.

However, all the current algorithms suffer from three drawbacks. A widely used assumption is that *refpos* distribute uniformly across the reference sequence, which results in the use of fixed bit coding for *refpos* compression. Another widely used assumption is that the distribution of mismatching positions (*mispos*) is also uniform. So they use difference to encode *mispos*. Finally, they do not consider the influence of continuous mismatching and design a simple matching model. The model sets a threshold for the mismatching count of the entire read. However, further analysis of the data reveals that both the distribution of *refpos* and *mispos* were non-uniform. It means all three models used before are improvable. Based on these, AMGC designed three modules targeting improving the three disadvantages.

3 Insight

Before the detailed introduction of the three modules of the proposed AMGC algorithm, we reveal two important properties of NGS sequencing process. It will help the reader to understand the technical motivation of the three key modules. In Section 3.1, we first review the pipeline of reference-based algorithms taking the integer-mapped k-mer indexing method (available at <http://www.ysunlab.org/kic.jsp>) as an example. And then we show the effect of each matching result on the final compressed size. In Sections 3.2 and 3.3, we simply review the process of NGS sequencing and the reaction of the synthesis, followed by a detailed analysis of the distribution of *refpos* and *mispos*.

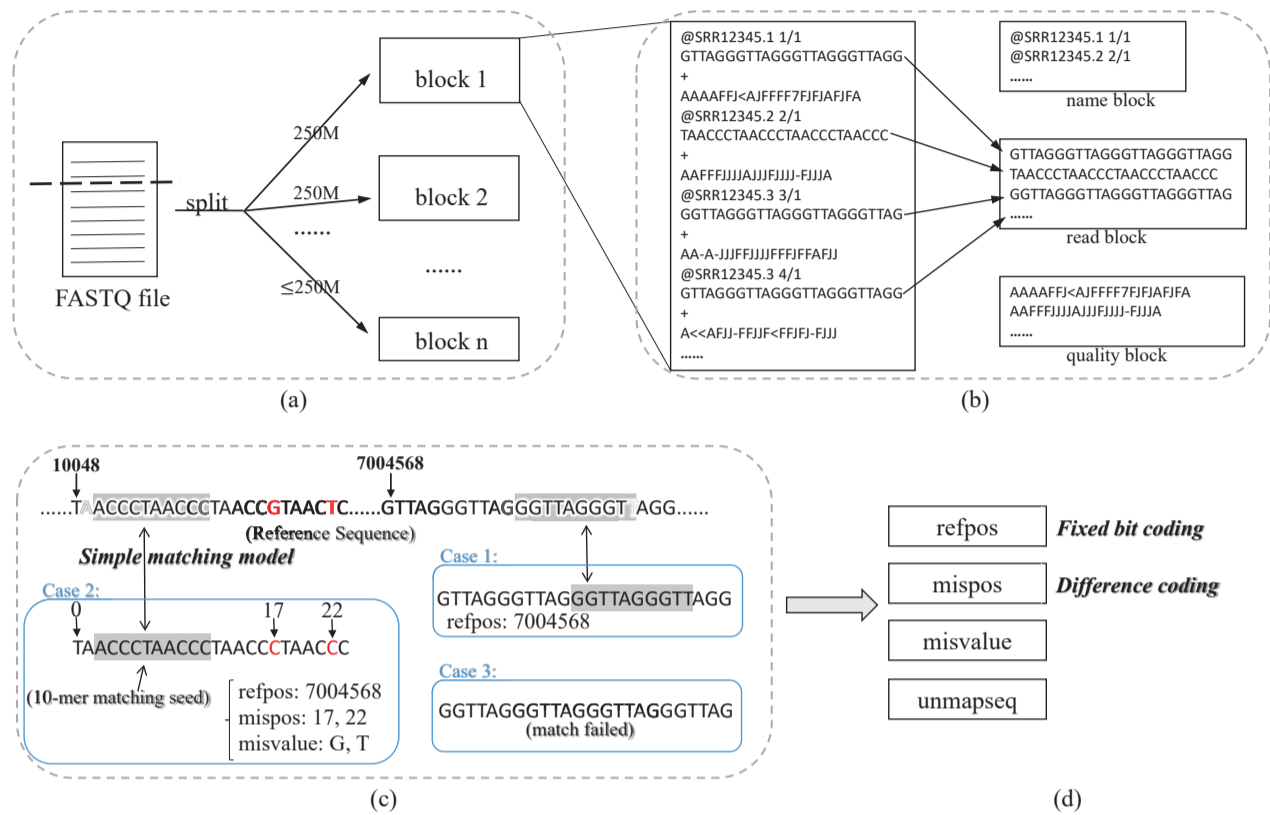


Fig. 1. The pipeline of reference-based algorithms. The bold italics are the three modules other compressors used, and AMGC's three modules are designed for improving them. The three blue boxes in (c) show the three cases of matching.

3.1 Pipeline of reference-based approaches

Notation: Let "refpos" represent the matching positions of each read on the reference sequence. Let "mispos" refer to the position of mismatching bases on read. Let "misvalue" represent the correct base on the reference sequence for each mismatch position. Let "unmapseq" refer to the set of reads that failed to match.

To begin, a FASTQ file is split into multiple 250MB memory blocks (as shown in Fig. 1(a)). This is necessary because FASTQ files are typically too large to be loaded into RAM at once. And splitting them enables easier multi-threaded processing. In Fig. 1(b), each 250MB block is further divided into "name block", "read block", and "quality block". Each 250MB block is unique, thus requiring adaptive encoding solutions for reads within different blocks.

Our focus is on the "read block". In Fig. 1(c), each read is aligned to the reference sequence one by one using the 10-mer integer model. Some read match perfectly (Case 1), and we only need to record their refpos. Some other reads match successfully but with a few different bases (Case 2), and we need to record their refpos, mispos, and misvalue. For the remaining reads (Case 3), the part in unmapseq, the match failed due to their large gap from all substrings in the reference sequence. More specifically, after determining the reference position by k-mer, it will expand to both ends and compare the bases at each corresponding position. If the number of different bases exceeds a certain threshold, the signal time alignment will be judged as a failure. When multiple k-mer mappings fail, read is judged as a match failure. After the matching process, the read block is transferred to the four parts in Fig. 1(d), and the only thing left is compression.

Fig. 2 presents the proportion of each part in a read block after matching. As shown, the "refpos", "unmapseq", and "mispos" components

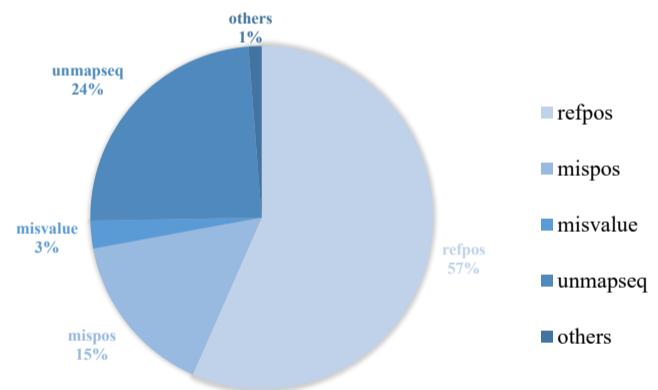


Fig. 2. The percentage of the size of each part in a read block after matching. The "others" category is about the processing of merger bases. The data used is from the first 50MB of data in the SRR6691666_1.fastq processed by AVS-G.

are critical factors in determining the size of the compressed data. To address this, AMGC has developed three modules to decrease compression size. The bit-plane-based differential refpos encoding module significantly reduces the size of "refpos" part. The recursive split matching module increases the number of successfully matched reads, thereby indirectly reducing the "unmapseq" part. Additionally, the adaptive binary mispos encoding module provides a new encoding method for "mispos".

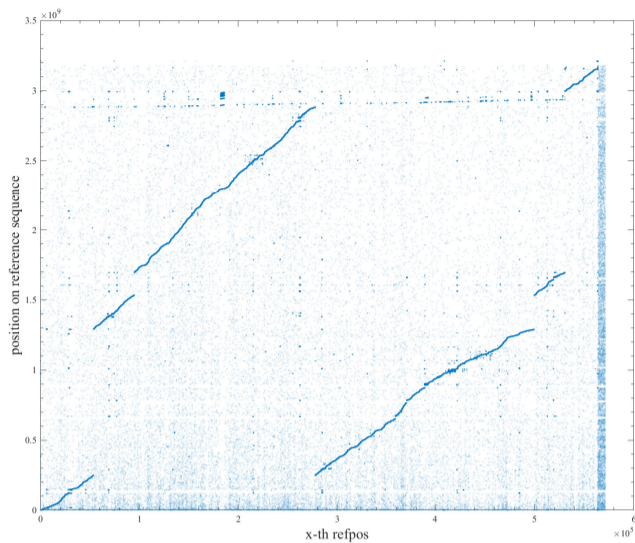


Fig. 3. Distribution of refpos for all the reads of FASTQ file in a Scatter plot. The horizontal axis represents each read, while the vertical axis represents the position in the reference file hg38.fa.

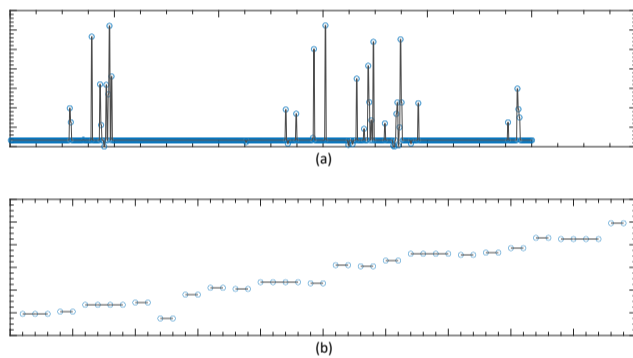


Fig. 4. Distribution of refpos for local reads of FASTQ file in a Scatter plot

3.2 Distribution of refpos

In the case of NGS, for example, the extracted DNA sample needs to be cut into small fragments during the sample preparation stage, then PCR amplifies the sample and aggregates it into Cluster before starting the synthetic sequencing session. The other strand paired with a fluorescently labelled deoxyribonucleotide of a different colour emits light signals of a different colour at the same time. These light signals are captured by the sequencer, which distinguishes different bases based on the different light signals and writes the sequencing results into a text file, such as a FASTQ file, to complete the sequencing process. The point is that as nearby small DNA fragments are sequenced, reads with similar positions in the FASTQ file are often matched to regions with similar positions, resulting in a strong local correlation in the comparison position information. Furthermore, since sequencing is done sequentially, the refpos of the reads in the FASTQ file are growing locally linearly too.

As shown in Fig. 3, a scatter plot of refpos for all the reads of SRR6178157 is presented. It can be observed that refpos is a one-dimensional signal with a locally growing trend and some noise. Hence, we can leverage this growth property to develop our refpos encoding module.

To have a closer view, we zoomed in on Fig. 3. As depicted in Fig. 4, each blue scatter represents a refpos, and the black line is used to aid

observation. With 1000 consecutive refpos in Fig. 4(a), it can be observed that the signal grows linearly while displaying some noise at a distance. With 50 consecutive refpos in Fig. 4(b), the black line segments indicate the same refpos in succession. The occurrence of consecutive identical refpos may result from the PCR process. These distribution characteristics of the refpos signal serve as the basis for AMGC’s design of the bit-plane-based differential refpos encoding module.

3.3 Distribution of mispos

Sequencing errors can introduce inaccuracies when comparing the resulting reads to the reference bases. To design a more effective compression algorithm, it’s important to analyze the sources of errors. During the early stages of the synthesis and sequencing process, the reaction may be unstable, but the quality of the DNA enzyme is good. However, as sequencing progresses, the reaction stabilizes while the enzyme activity and specificity gradually decline, leading to cumulative errors that increase over time. This trend results in a slight decrease in the error rate of base sequencing followed by an increase after stabilization. Further analysis of this phenomenon is available in (Minoche et al. (2011)).

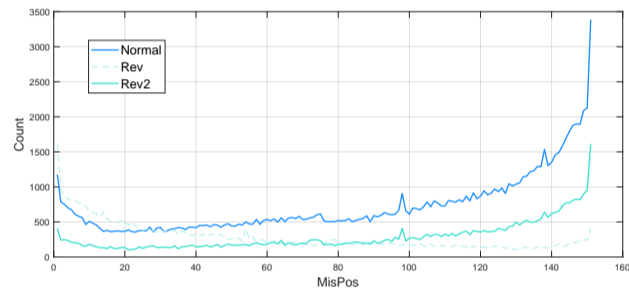


Fig. 5. Distribution of mispos for the read in a Scatter plot. The horizontal axis indicates each position, while the vertical axis displays the number of errors. The two different lines, ‘Normal’ and ‘Rev’, represent the sequential and reverse comparisons, respectively. We also display ‘Rev2’, which is the reverse of ‘Rev’.

Fig. 5 displays the distribution of mispos in a scatter plot for 143003 reads in the FASTQ file “SRR6178157.fastq”. It clearly shows the trend analyzed above. To address this feature, we design the adaptive binary mispos encoding module. We also carefully consider the effects of these mismatched bases on the matching process and come out with the recursive split matching module.

4 Methods

After providing the technical motivation for the three modules, this section delves into their implementation details. In Section 4.1, we describe the entire process of refpos processing, including the use of deduplication, differential, and median filtering to fit the observed data features of refpos. In Section 4.2, we introduce the adaptive binary mispos encoding module, which uses a binary vector to represent matching mistakes and then uses a high-order context to encode the vector. In Section 4.3, we introduce the recursive split matching module to enable high-quality subsegment on unmapped reads matches.

4.1 Bit-plane-based differential refpos encoding

Existing approaches do not consider the distribution of refpos. We use the difference operation to account for the significant local correlation of the refpos. Median filtering is used in the differencing process taking into

account the noise points. The median filtering difference formula is :

$$d(x) = p(x) - \text{mid} \{p(x-1), p(x-2), p(x-3)\}$$

where $p(x)$ represents the x -th *refpos* and $d(x)$ represents the x -th *refpos* after differencing, "mid" represent the median of three numbers, $p(0)$, $p(-1)$ and $p(-2)$ are zeros. We will first eliminate consecutive repetitions of the *refpos* to fit the character that the same *refpos* will display continually.

The input for this technology is the "refpos" part after matching. As an example, we use the human genome and hg38.fa, where each *refpos* represents 32 bits. Here are the steps involved in this technology:

- Step 1: Remove consecutive duplicates of *refpos*. Our analysis revealed that there were numerous instances of some consecutive *refpos* being identical. This might be due to two identical readings being combined, and the duplicates were eliminated in the initial stage of processing the *refpos*. We put the description of the duplicates in the "PosEqual" file, where 1 denotes that it is the same as the prior *refpos*, and 0 denotes that it is different. To encode "PosEqual", we use a binary arithmetic encoder.
- Step 2: Perform median filtering difference on the processed *refpos*. In Section 3, we observe the linear growth property of *refpos* due to the DNA chain order sequencing. To process this one-dimensional signal, we apply differencing. Due to the presence of noise, the difference is disturbed and we use the median of the first three *refpos* of the current *refpos* as the subtracted number to filter out the noise.

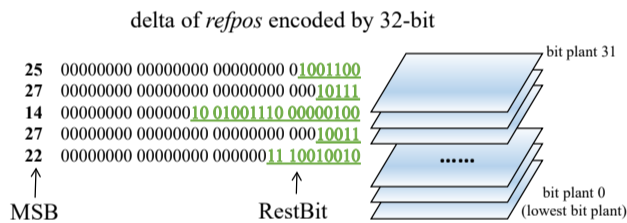


Fig. 6. Encoding algorithm of *refpos* delta. The right figure shows what is bit plant. The left figure shows how to separate *refpos* delta to "MSB" (most significant bit) and "RestBit"

- Step 3: Encode the differential result into bit planes. We represent the diff result as a positive or negative sign and 32-bit planes, which are split into "MSB" (most significant bit) and "RestBit" parts (Fig. 6). The sign part will be put into a simple arithmetic encoding model. For the "MSB" part, we use the 32-value arithmetic encoder to encode directly. For the "LeftBit" part, the MSB and the bit plane where each bit is located are used as the context when encoding.

4.2 Adaptive binary *mispos* encoding

Considering the distribution of *mispos* on read is not uniform, we use a higher-order context encoding to capture the relevance of the mismatch trend. The input of this technology is the "*mispos*" part after matching. We use 151-mer read as an example.

- Step 1: A binary vector is utilized to denote a matching mistake. According to the analysis in Section Insight, the error probability of each base in the read is not uniform, and the error probability of the tail part is higher. Therefore, we separate each position and then encode the error positions with the binary signal as shown in Fig. 7.
- Step 2: Use higher-order context encoding. To capture the relevance of the mismatch trend, instead of simply encoding each bit with the

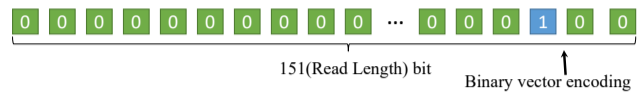


Fig. 7. Binary signal of *mispos*

position as context, AMGC employs the number of errors in the first 10 bases of the current bit position as context. The probabilistic way of modelling the current encoded bit:

$$p \left(x_i \mid \sum_{k=i-10}^{i-1} x_k \right)$$

4.3 Recursive divide matching

This technology is used in the matching process. Taking the integer-mapped k -mer indexing method as an example, mapping tools will match the read into the reference sequence through the short k -mer on read, and then expend k -mer to the entire read. If the number of mismatched bases exceeds the threshold, expending ends and matching fail. However, as analyzed in section 3.3, sequencing errors are more likely to occur at the end of the read. That means the high-quality segment in the front of the read is also thrown into the *unmapseq* part, causing a waste of reference sequence.

To address this, our recursive divide matching technology cuts the matching failed read into two equal segments and puts them into mapping tools again until they are too short to split. The splitting process runs recursively until the subsegment is shorter than a threshold.

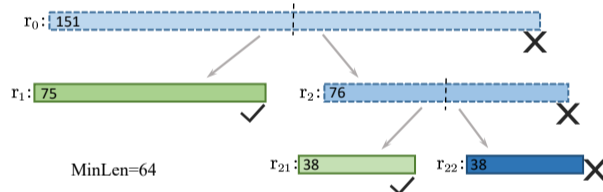


Fig. 8. Matching case of input read and its subsegments. Everyone will only be split into two equal-length parts from the middle. The nation, "right" or "wrong" represents matching success or failure. "MinLen" is the threshold stopping recursive dividing.

As shown in Fig. 8, the input read (r_0) has a length of 151. After its matching failed, we split it into two equal-length parts (r_1 with length 75 and r_2 with length 76). As the sequencing errors are more likely to occur at the end of the read, r_1 matches successfully and r_2 matches fail. We then divide r_2 into r_{21} (length 38) and r_{22} (length 38). r_{21} matches successfully and r_{22} matches fail, but r_{22} is too short to divide further. The whole matching of r_0 ends and we successfully decrease the unmapped base count and reduce the size of *unmapseq* by making better usage of the reference sequence.

5 Results and Discussion

The proposed algorithm, AMGC, was evaluated using *AVS-G* as it is an accessible software for us, and then tested on various real datasets. In the following, we will use "AMGC" to refer to both the algorithm and the compressor *AVS-G* with our algorithm deployed. AMGC's performance was compared to various existing algorithms. We tested the performance against GTZ, Leon, HARC, PgRC and gzip. GTZ is a very widely used

Table 1. Datasets used for compression

Dataset	Original size	RUN	Species name	Technology	Platform	SE/PE	Read length
SRR4017489_1	16.5 GB	SRR4017489	Homo sapiens	WCS	Illumina HiSeq 2000	PE	101,101
SRR6691666_1	316.1 GB	SRR6691666	Homo sapiens	WGS	TruSeq + Illumina HiSeq X	PE	151,151
ERR753370_1	12.7 GB	ERR753370	Homo sapiens	FINISHING	Illumina HiScanSQ	PE	101,101
SRR1238539	74.2 GB	SRR1238539	Homo sapiens	WGS	Ion Torrent Proton	SE	177
SRR6178157	37.0 GB	SRR6178157	Homo sapiens	WXS	Ion Torrent Proton	SE	135
SRR3479107	5.9 GB	SRR3479107	Mus musculus	MBD-Seq	AB 5500xl Genetic Analyzer	PE+SE	30,30
SRR3479107_1	21.9 GB						
SRR5572323	29.8 GB	SRR5572323	Mus musculus	FAIRE-seq	Illumina HiSeq 2000	SE	76
SRR6240776	8.5 GB	SRR6240776	Arabidopsis thaliana	ATAC-Seq	Illumina HiSeq 4000	PE+SE	50, 50
SRR6240776_1	14.9 GB						

Notes: _1 denotes that only one out of the two paired-end FASTQ files was used. RUNs with both SE and PE share some common information.

Table 2. Performance of compressors

Dataset	Original size	Length	Compression ratio							Gain
			GTZ	LEON	HARC	PgRC	gzip	AVS-G	AMGC	
SRR4017489_1	16.5GB	101,101	81.82	23.40	30.08	77.47	19.30	51.64	147.82	80.66%
SRR6691666_1	316.1GB	151,151	73.51	24.70	60.79	81.05	16.81	53.56	98.78	21.88%
ERR753370_1	12.7GB	101,101	73.89	22.22	-	-	15.37	53.45	121.20	64.03%
SRR1238539	74.2GB	~177	19.53	8.83	-	-	11.78	10.78	21.82	11.73%
SRR6178157	37.0GB	~135	17.62	11.56	-	-	11.21	14.29	19.47	10.50%
SRR3479107	5.9GB	30,30	15.28	13.63	13.87	18.42	7.51	25.64	77.96	204.06%
SRR3479107_1	21.9GB	30	14.60	13.69	15.64	24.80	8.42	25.26	72.81	188.24%
SRR5572323	29.8GB	76	45.92	11.46	14.90	24.83	9.93	34.66	68.14	48.39%
SRR6240776	8.5GB	~50	17.36	16.50	-	-	6.07	19.08	21.56	13.00%
SRR6240776_1	14.9GB	~50,~50	29.55	29.07	-	-	15.60	43.67	117.82	169.80%
Average gain over the second-best-performing compressors:									81.23%	

Notes: For data with different Read Lengths, HARC and PgRC compression failed. The compression ratio is obtained by $total\ size/compression\ size$. Given the extremely small percentage of identifiers, the true read compression ratio is about half of the compression ratio given.

compressor nowadays. Its reference compression mode has a very high compression ratio and compression efficiency. We only test the reference compression mode of GTZ and do not package the used reference part (-r -n). Leon, HARC and PgRC are three representative assembly-based methods. They use different ways of splicing reference genes. Gzip is the classical universal compressor. The tests were run on a machine with an 11th Gen Intel Core i7-11700F 2.50 GHz processor and 128 GB of RAM.

5.1 Datasets

The datasets used for evaluation were chosen from the standard test datasets provided by AVS-G, which are listed in Table 1. These datasets consist of five Homo sapiens, two Arabidopsis thaliana, and three Mus musculus and include information on the raw sizes, read lengths, sequencing platforms, and sequencing methods used.

Our main targets for comparison are GTZ, AVS-G and AMGC. Since our algorithm focuses only on compressing the read part, we preprocessed the FASTQ files before testing. We simplified the identifier part and set the quality values to the same value, enabling our test results to focus on the read part. As the processing of the different parts in GTZ is integrated, we include the identifiers and quality values parts in the compression output, but this does not affect the comparison between GTZ, AVS-G, and AMGC. It should be noticed that the experiments are conducted in a way which favours the assembly-based algorithms. Because the formatted identifiers

and quality values still have a slight impact on GTZ, AVS-G, and AMGC, assembly-based algorithms throw them.

5.2 Compression size and ratio

Table 2 illustrated the compression ratio for different compression tools. We highlighted the best-performing compressors in red and the second-best-performing compressors in blue. It was evident from the table that GTZ and AVS-G had their advantages in different data and were currently the two top compressors. PgRC was the best compressor among assembly-based compressors. It got the second-best performance when compressing data SRR6691666_1. However, AMGC outperformed all other compressors, achieving an average compression ratio that was 81.23% higher than the second-best-performing compressor.

5.3 Time and memory usage

Tables 3 and Tables 4 presented the time and memory usage for compression and decompression. All compressors were run with sixteen threads. For compressors that compressed the whole FASTQ files, the quality values did less impart on compress ratio but still occupied corresponding memory because of the preprocess of FASTQ files.

The reference-based compressors, such as AVS-G and GTZ, showed better time usage when compressing and decompressing. Assembly-based

Table 3. Time usage of compressors

Dataset	Original size	Encoding Time							Decoding Time						
		GTZ	LEON	HARC	PgRC	gzip	AVS-G	AMGC	GTZ	LEON	HARC	PgRC	gzip	AVS-G	AMGC
SRR4017489_1	16.5 GB	2m7s	3m47s	5m56s	5m46s	4m8s	3m5s	3m19s	23s	1m20s	41s	17s	39s	1m18s	1m22s
SRR6691666_1	316.1 GB	21m18s	126m9s	149m9s	294m5s	65m51s	36m49s	41m33s	21m33s	45m23s	32m6s	13m2s	35m37s	32m52s	32m59s
ERR753370_1	12.7 GB	2m34s	3m20s	-	-	3m42s	1m40s	1m47s	2m5s	1m1s	-	-	31s	16s	17s
SRR1238539	74.2 GB	9m31s	41m24s	-	-	20m10s	4m55s	17m47s	13m6s	12m53s	-	-	4m18s	5m33s	5m31s
SRR6178157	37.0 GB	5m39s	11m58s	-	-	9m42s	4m0s	7m5s	6m30s	4m3s	-	-	1m40s	1m22s	1m25s
SRR3479107	5.9 GB	56s	53s	13m7s	3m44s	3m19s	1m55s	1m15s	11s	35s	22s	19s	17s	10s	14s
SRR3479107_1	21.9 GB	2m0s	2m47s	78m15s	11m30s	7m57s	1m50s	2m2s	42s	3m20s	42s	57s	1m2s	34s	44s
SRR5572323	29.8 GB	3m24s	8m33s	16m47s	21m22s	10m45s	3m22s	3m8s	1m4s	3m28s	2m15s	1m19s	1m21s	1m52s	1m54s
SRR6240776	8.5 GB	1m10s	1m55s	-	-	5m44s	47s	33s	1m20s	59s	-	-	26s	14s	16s
SRR6240776_1	14.9 GB	1m24s	2m26s	-	-	3m14s	1m31s	1m10s	1m53s	1m44s	-	-	36s	16s	19s

Notes: For data with different Read Lengths, HARC and PgRC compression failed.

Table 4. Memory usage of compressors

Dataset	Original size	Encoding RAM							Decoding RAM						
		GTZ	LEON	HARC	PgRC	gzip	AVS-G	AMGC	GTZ	LEON	HARC	PgRC	gzip	AVS-G	AMGC
SRR4017489_1	16.5 GB	4.0G	4.8G	3.3G	3.4G	1.7M	9.5G	23.4G	9.0G	1.4G	0.4G	2.2G	1.4M	5.4G	8.4G
SRR6691666_1	316.1 GB	6.4G	7.9G	47.8G	72.3G	1.6M	13.9G	34.7G	9.6G	13.2G	1.9G	24.7G	1.5M	5.5G	23.9G
ERR753370_1	12.7 GB	5.7G	0.9G	-	-	1.6M	8.9G	21.1G	17.4G	1.4G	-	-	1.4M	4.0G	9.4G
SRR1238539	74.2 GB	9.3G	6.1G	-	-	1.8M	11.7G	23.0G	19.4G	8.0G	-	-	1.4M	3.7G	11.8G
SRR6178157	37.0 GB	8.9G	2.5G	-	-	1.7M	8.8G	22.6G	18.6G	3.5G	-	-	1.4M	3.9G	12.0G
SRR3479107	5.9 GB	3.3G	0.5G	0.9G	3.3G	1.6M	17.0G	18.2G	7.1G	0.6G	0.3G	1.7G	1.5M	3.2G	9.4G
SRR3479107_1	21.9 GB	4.4G	1.7G	6.5G	11.6G	1.8M	9.5G	17.4G	9.4G	6.1G	0.5G	4.3G	1.5M	4.4G	13.0G
SRR5572323	29.8 GB	6.9G	2.2G	9.2G	10.0G	1.7M	12.4G	29.9G	8.6G	2.7G	0.9G	4.5G	1.4M	5.2G	16.3G
SRR6240776	8.5 GB	7.6G	0.5G	-	-	1.6M	6.6G	12.0G	12.4G	1.2G	-	-	1.3M	2.7G	8.7G
SRR6240776_1	14.9 GB	6.1G	0.7G	-	-	1.7M	3.1G	14.4G	16.1G	0.4G	-	-	1.4M	3.3G	10.8G

Notes: For data with different Read Lengths, HARC and PgRC compression failed.

compressors required more time to assemble all input reads into a sequence when compressing, resulting in higher time usage. Compared to AVS-G, AMGC had a similar time complexity, which meant our algorithm did not significantly increase the time required.

A special example was SRR1238539 from the Ion Torrent Proton platform, where AMGC used more compression time than AVS-G. This was because reads from this platform may be longer than normal NGS reads. The recursive split matching module of AMGC required more alignment times for longer reads, resulting in longer encoding times. However, our algorithm was stable with other data sets. When compared to GTZ, AMGC performs similarly in compression but better in decompression.

In terms of memory consumption, GTZ and Leon were efficient while gzip had a notable advantage. When dealing with large-size data, HARC and PgRC used a lot of memory. AMGC had higher overall memory usage. However, with the development of memory technology, larger memory has become widely available, and the amount of memory used is no longer a significant factor in determining the strengths and weaknesses of genomic compression algorithms, but the compression ratio is.

5.4 Discussion

Even though assembly-based compression algorithms do not require an external reference sequence, the process of read matching exists after assembling their reference sequence. Therefore, our algorithm is suitable for both kinds of methods.

Overall, AMGC gets an 81.23% gain compared with the second-best-performing compressors with comparable RAM and time usage. This is significant work in lossless compression.

6 Conclusion and future work

We have introduced AMGC, a new algorithm that includes three modules to boost the compression of reads based on read matching. This algorithm can be integrated into various genomic compression tools. AMGC outperformed state-of-the-art methods and gets an 81.23% gain compared to the second-best-performing compressor.

Future work could involve extending AMGC to the compression of spatial omics genomic data by developing a more suitable k-mer mapping tool and incorporating spatial omics information into the encoding of mapping results.

Funding

This work has been supported by NSFC 61875157 and an open project of BGI-Shenzhen, Shenzhen518000, China.

References

- Benoit, G. *et al.* (2015). Reference-free compression of high throughput sequencing data with a probabilistic de bruijn graph. *BMC bioinformatics*, **16**(1), 1–14.
- Bonfield, J. K. and Mahoney, M. V. (2013). Compression of fastq and sam format sequencing data. *PLoS one*, **8**(3), e59190.
- Burrows, M. and Wheeler, D. (1994). A block-sorting lossless data compression algorithm. In *Digital SRC Research Report*. Citeseer.
- Chandak, S. *et al.* (2018). Compression of genomic sequencing reads via hash-based reordering: algorithm and analysis. *Bioinformatics*, **34**(4), 558–567.

- Deorowicz, S. and Grabowski, S. (2011). Compression of genomic sequences in fastq format. *Bioinformatics*, **27**(6), 860–862.
- Fritz, M. H.-Y. et al. (2011). Efficient storage of high throughput dna sequencing data using reference-based compression. *Genome research*, **21**(5), 734–740.
- Jones, D. C. et al. (2012). Compression of next-generation sequencing reads aided by highly efficient de novo assembly. *Nucleic acids research*, **40**(22), e171–e171.
- Kowalski, T. M. and Grabowski, S. (2020). Pgrc: pseudogenome-based read compressor. *Bioinformatics*, **36**(7), 2082–2089.
- Lander, E. et al. (2001). Initial sequencing and analysis of the human genome. *Nature*, **409**.
- Li, H. (2013). Aligning sequence reads, clone sequences and assembly contigs with bwa-mem. *arXiv preprint arXiv:1303.3997*.
- Li, H. et al. (2009). The sequence alignment/map format and samtools. *bioinformatics*, **25**(16), 2078–2079.
- Ma, X. et al. (2019). Analysis of error profiles in deep next-generation sequencing data. *Genome biology*, **20**, 1–15.
- Mardis, E. R. (2008). Next-generation dna sequencing methods. *Annu. Rev. Genomics Hum. Genet.*, **9**, 387–402.
- Minoche, A. E. et al. (2011). Evaluation of genomic high-throughput sequencing data generated on illumina hiseq and genome analyzer systems. *Genome biology*, **12**(11), 1–15.
- Niu, Y. et al. (2022). Aco: lossless quality score compression based on adaptive coding order. *BMC bioinformatics*, **23**(1), 1–14.
- Schadt, E. E. et al. (2010). A window into third-generation sequencing. *Human molecular genetics*, **19**(R2), R227–R240.
- Wee, Y. et al. (2019). The bioinformatics tools for the genome assembly and analysis based on third-generation sequencing. *Briefings in functional genomics*, **18**(1), 1–12.
- Xing, Y. et al. (2017). Gtz: a fast compression and cloud transmission tool optimized for fastq files. *BMC bioinformatics*, **18**(16), 233–242.
- Zhang, Y. et al. (2015). Light-weight reference-based compression of fastq data. *BMC bioinformatics*, **16**(1), 1–8.
- Ziv, J. and Lempel, A. (1977). A universal algorithm for sequential data compression. *IEEE Transactions on information theory*, **23**(3), 337–343.